Brief Definitive Report

The Exocytosis-regulatory Protein Synaptotagmin VII Mediates Cell Invasion by *Trypanosoma cruzi*

By Elisabet V. Caler, Sabyasachi Chakrabarti, Kimberly T. Fowler, Swathi Rao, and Norma W. Andrews

From the Section of Microbial Pathogenesis, Boyer Center for Molecular Medicine, Yale University School of Medicine, New Haven, Connecticut 06520

Abstract

The intracellular protozoan parasite *Trypanosoma cruzi* causes Chagas' disease, which affects millions of people in Latin America. *T. cruzi* enters a large number of cell types by an unusual mechanism that involves Ca^{2+}-triggered fusion of lysosomes with the plasma membrane. Here we show that synaptotagmin VII (Syt VII), a ubiquitously expressed synaptotagmin isoform that regulates exocytosis of lysosomes, is localized on the membranes of intracellular vacuoles containing *T. cruzi*. Antibodies against the C_2A domain of Syt VII or recombinant peptides including this domain inhibit cell entry by *T. cruzi*, but not by *Toxoplasma gondii* or *Salmonella typhimurium*. The C_2A domains of other ubiquitously expressed synaptotagmin isoforms have no effect on *T. cruzi* invasion, and mutation of critical residues on Syt VII C_2A abolish its inhibitory activity. These findings indicate that *T. cruzi* exploits the Syt VII–dependent, Ca^{2+}-regulated lysosomal exocytic pathway for invading host cells.

Key words: trypanosome • parasite • intracellular • secretion • calcium

Introduction

Human infection with *Trypanosoma cruzi* is prevalent in extensive areas of South and Central America, where more than 15 million people are estimated to be chronically infected. The acute phase of the infection is often fatal in children, and survivors frequently develop serious conditions such as cardiomyopathy and megacolon, which can lead to premature death. A large number of wild animals serve as reservoirs for *T. cruzi*, and this broad host range correlates well with the parasite's ability to invade and replicate inside a large variety of mammalian cell types.

Previous studies revealed that infection of fibroblasts and epithelial cells by trypomastigotes, the infective forms of *T. cruzi,* occurs by an unusual mechanism, distinct from phagocytosis. Parasite entry is independent of host cell actin polymerization and requires mobilization of host cell lysosomes to the invasion site (1, 2). Time-lapse imaging of the invasion process revealed a directional movement and clustering of lysosomes at the site of trypomastigote attachment, followed by progressive fusion of lysosomes with the plasma membrane as the parasites entered the cell (3). Recently and partially internalized trypomastigotes are found in acidic intracellular vacuoles containing lysosomal markers, strongly suggesting that the parasite-containing compartment is formed through lysosomal fusion (2). A trypomastigote-triggered signaling cascade resulting in a localized elevation of the host cell intracellular free Ca^{2+} concentration ($[Ca^{2+}]_i$) is also required for cell invasion and for the efficient establishment of infections in mice (4–7). Thus, the *T. cruzi* cell entry process has several features that resemble regulated exocytosis: it involves elevation in $[Ca^{2+}]_i$ and mobilization of lysosomes to the plasma membrane, followed by fusion.

The similarities between the *T. cruzi* invasion process and regulated exocytosis led us to investigate a possible role for synaptotagmin VII (Syt VII), a ubiquitously expressed member of the synaptotagmin family previously implicated in the regulation of lysosomal exocytosis (8). Synaptotagmins are transmembrane proteins with a short NH_2-terminal ectodomain, a single transmembrane region, and two highly conserved, independently folding Ca^{2+}-binding C_2 domains (C_2A and C_2B) homologous to the C_2 regulatory region of protein kinase C. Genetic studies in mice, *Drosophila*, and *Caenorhabditi elegans* revealed that synaptotagmin I (Syt I), which is present on the membranes of synaptic vesicles in neurons, is essential for normal Ca^{2+}-dependent neurotransmitter release (9, 10). The C_2A domains of Syt I and of several additional isoforms interact with the

Address correspondence to Norma W. Andrews, Section of Microbial Pathogenesis, Boyer Center for Molecular Medicine, Yale University School of Medicine, 295 Congress Ave., New Haven, CT 06536. Phone: 203-737-2410; Fax: 203-737-2630; E-mail: norma.andrews@yale.edu

 J. Exp. Med. © The Rockefeller University Press • 0022-1007/2001/05/1097/08 $5.00
Volume 193, Number 9, May 7, 2001 1097–1104
http://www.jem.org/cgi/content/full/193/9/1097

t-SNARE (soluble *N*-ethylmaleimide–sensitive factor attachment protein receptor) syntaxin and with acidic phospholipids in a Ca^{2+}-dependent manner, albeit with slightly different properties (11). A Ca^{2+}-dependent interaction was also detected between the C_2A domain of Syt I and SNAP-25 (12), another core component of the conserved SNARE membrane fusion "machine" (13). Although several of the 12 rat and mouse synaptotagmin isoforms described to date are primarily found in brain, some are also expressed in other tissues (11, 14). Syt VII, in particular, is expressed at significant levels on most mouse tissues (15). Consistent with this ubiquitous pattern of expression, recent work from our laboratory showed that Syt VII is localized on the membrane of lysosomes in NRK cells (8).

Recently proposed models for the role of Syt I in synaptic vesicle exocytosis suggest that Ca^{2+}-triggered interactions involving the C_2 domains alter the physical relationship between the SNARE complex and the lipid bilayers, facilitating fusion (12, 16). In particular, several lines of evidence indicate that the C_2A domain is central for the function of synaptotagmins in the regulation of Ca^{2+}-triggered exocytosis (12, 17–20). Antibodies generated against the Syt I C_2A domain and recombinant peptides containing the Syt I C_2A domain are powerful inhibitors of Ca^{2+}-triggered exocytosis when introduced into neuronal cells (18–20). Similarly, the C_2A domain of Syt VII or antibodies to this domain efficiently block Ca^{2+}-triggered exocytosis of lysosomes in permeabilized NRK cells (8). Importantly, inhibition of lysosomal exocytosis in NRK cells is only observed in the presence of the Syt VII C_2A domain, and not the C_2A domain of the exclusively neuronal isoform Syt I (8). These observations indicate that Syt VII functions as a specific regulator of lysosomal exocytosis, which is triggered at low micromolar $[Ca^{2+}]_i$ in several cell types (21–23). In this report, we show that modulation of Syt VII function inhibits host cell invasion by *T. cruzi*, strongly suggesting that this parasite utilizes the Ca^{2+}-regulated lysosomal exocytic pathway for establishing intracellular infections.

Materials and Methods

Antibodies, Western Blot, and Immunofluorescence. Polyclonal antibodies against the Syt VII NH_2-terminal ectodomain were generated by immunization of a rabbit with the synthetic peptide MYRDPEAASPGAC and purified as described previously (8). Rabbit polyclonal antibodies against *Escherichia coli*–expressed Syt VII C_2A domain were also generated and affinity purified as previously described (8). For Western blots, extracts of NRK (rat), Hela, HEK-293 (human), 3T3 (mouse), and CHO (hamster) cells were prepared in 150 mM NaCl, 50 mM Tris, pH 8.6, and 1% NP-40 containing protease inhibitors. 20 μg of cell extract was loaded on each lane for SDS-PAGE, transferred to immobilon filters, and probed with purified anti–Syt VII IgG followed by ECL (New England Nuclear) detection (9). Immunofluorescence assays were performed on HEK-293 and 3T3 cells fixed in 100% methanol at 20°C for 10 min and rehydrated in PBS for 30 min, followed by anti–Syt VII rabbit IgG (8) and a mouse mAb to human Lamp-1 (H4A3) or a rat mAb to mouse Lamp-1 (1D4B; Developmental Studies Hybridoma Bank, Iowa City, IA). CHO cells were fixed in 2% paraformaldehyde, incubated for 15 min in 50 mM NH_4Cl, permeabilized with 0.1% Triton X-100 for 30 min, and incubated with rabbit anti–Syt VII and a mouse mAb to hamster Lamp-1 (UH1), followed by the appropriate secondary antibodies (goat anti-rabbit, -mouse, or -rat conjugated to Alexa 488 or 546; Molecular Probes). Images were acquired in a Zeiss Axiovert 135 microscope through a 100× objective using a Hamamatsu Orca II cooled CCD camera, controlled by Metamorph software (Universal Imaging).

Reverse Transcription PCR, Site-directed Mutagenesis, and Transfections. cDNA was synthesized from 10 μg of total RNA previously treated with Rnase-free Dnase I (GIBCO BRL). Forward and reverse primers used for reverse transcription (RT)-PCR amplification of the synaptotagmin C_2A domains were designed based on nonconserved regions encoded by two separate exons of the individual rat DNA sequences and were as follows: 5′-GAGGAGAAACTGGGAAAGCTC-3′ (forward) and 5′-TTTCTCAGCGCTCTGGAGAT-3′ (reverse) for Syt I C_2A, 5′-GAAAGAGCCGGAGAACCTGG-3′ (forward) and 5′-ATTCCTCGATGGGCTGGCCAAG-3′ (reverse) for Syt II C_2A, 5′-CTTGCCCAGTGCCCAGTCTCATC-3′ (forward) and 5′-AGAGTGGACGGTCAGGGGGCTGTTC-3′ (reverse) for Syt III C_2A, 5′-CAAGAGAAGCTGGGCACTCTC-3′ (forward) and 5′-GGTCATTAACATTTTCCCGTCTGAC-3′ (reverse) for Syt IV C_2A, 5′-GCAAGAGCTGTGGGAAGATCAAC-3′ (forward) and 5′-AGATGGAGGTCTCCCGGGAC-3′ (reverse) for Syt VI C_2A, 5′-AGCCGAGAGAACCTG-3′ (forward) and 5′-ATGGGAGTGGGAGCCGAG-3′ (reverse) for Syt VII C_2A, 5′-TGCTCTGGAGGGGACCAACAG-3′ (forward) and 5′-ACCAGCTCTCCAGGACATGTTG-3′ (reverse) for Syt VIII C_2A, and 5′-CAGGTATTGGACAAGCACCAG-3′ (forward) and 5′-TGAACTCATAGGCACCCGCAC-3′ (reverse) for Syt IX C_2A.

The amplified products were first cloned into blunt-ended pBluescript plasmid and then into the EcoRI site of the pEGFP-N2 vector (Clontech). PCR-based site-directed mutagenesis reactions (Stratagene) were used to generate point mutations in the Syt VII C_2A domain, using the C_2A–pEGFP fusion plasmid as template. For mutations of aspartate residues to asparagines (D166N/D172N/D225N/D227N), two rounds of PCR mutagenesis were done using the following primers: 5′-AGGCCCAGGAGCTGCCGGCCAAGAACTTCAGTGGCACTAGTAACCCCTTTGTCAAGATCTACC-3′ and 5′-TCCGGGTCCTCGACGGCCGGTTCTTGAAGTCACCGTGATCATTGGGGAAACAGTTCTAGATGG-3′ for the first round and 5′-TCTACCTCCAGGTCCTGAACTATACCGTTTCAGCCGCAATG-3′ and 5′-AGATGGAGGTCCAGGACTTGATATTGGCAAAGTCGGCGTAC-3′ for the second round. The plasmid harboring the aspartate mutations was then used as template to replace the KKHK domain (K183A/K184A/H185A/K186A) using the following primers: 5′-ATCTACCTACTACCCGACGCGGCGGCGGCGCTGGAGACCAAGGTGAAAC-3′ and 5′-TAGATGGATGATGGGCTGCGCCGCCGCCGCGACCTCTGGTTCCACTTTG-3′. All C_2A–green fluorescent protein (GFP) mutant constructs were checked by sequencing and transiently expressed for functional studies.

Cell transfections were performed with 2 μg total DNA using FuGENE 6 (Boehringer Mannheim) on cells plated at 50% confluency 24 h before. Infections with *T. cruzi*, *Toxoplasma*, or *Salmonella* were done 24 h after transfection, when the fraction of cells showing cytosolic expression of GFP was ~20–30%.

Quantitation of GFP Expression Levels. The average GFP fluorescence intensity associated with transfected cells was measured on 8-bit data mode images acquired through a 100× objective with a Hamamatsu Orca II cooled CCD camera, controlled by Metamorph imaging software (Universal Imaging). The focal plane and outline of each cell was initially established by phase–contrast observations. Fluorescent images were acquired for 50 ms without autoscale, under conditions that ensured linear dynamic range detection of E-GFP emission at 507 nm. Individual cells on the images were outlined, and average fluorescence intensity values for each outlined region were obtained using the Metamorph "region statistics" function. Background fluorescence intensity values were acquired in an identical area of the same microscopic field containing no transfected cells and substrated from each value obtained for transfected cells. For each transfection group (GFPv, Syt I C_2A–GFP, Syt VII C_2A–GFP, Syt VIII C_2A–GFP, Syt IX C_2A–GFP, and mutated Syt VII C_2A–GFP [mSyt VII C_2A]), measurements were made in 40 randomly chosen individual cells. Cells expressing very high or very low levels of GFP, previously determined by eye examination, were excluded from the analysis.

Glass Bead Antibody Loading. Confluent monolayers of NRK cells were plated on 12-mm round coverslips 48 h before the experiment. Coverslips were rinsed in PBS^{2+} (containing Ca^{2+} and Mg^{2+}) on a heated stage at 37°C and covered with 50 μl of PBS^{2+} containing 5 mg/ml Texas Red–dextran and 20 μg/ml affinity-purified rabbit anti–Syt VII C_2A or preimmune rabbit IgG. The cells were then sprinkled with 0.05 g (~200 beads) of acid-washed glass beads (425–600 μm; Sigma-Aldrich) from a culture tube held 1–3 cm above the coverslip (24). The coverslips were gently rocked four times to let the beads roll over the cells, rinsed in PBS^{2+}, and exposed to *T. cruzi* trypomastigotes.

Microinjection. Microinjection of NRK and CHO cells was performed on a Zeiss Axiovert 135 microscope equipped with a heated stage, using an Eppendorf micromanipulator 5170 and microinjector 5242. Histidine (his)-tagged constructs of Syt VII and Syt I C_2A were expressed in *E. coli*, purified (8), and concentrated to 1 mg/ml in microinjection buffer (27 mM K_2HPO_4, 8 mM Na_2HPO_4, and 26 mM KH_2PO_4, pH 7.2) containing 1 mg/ml 10,000 MW Texas Red–dextran to visualize injected cells. Approximately 500 cells were microinjected in each experiment,

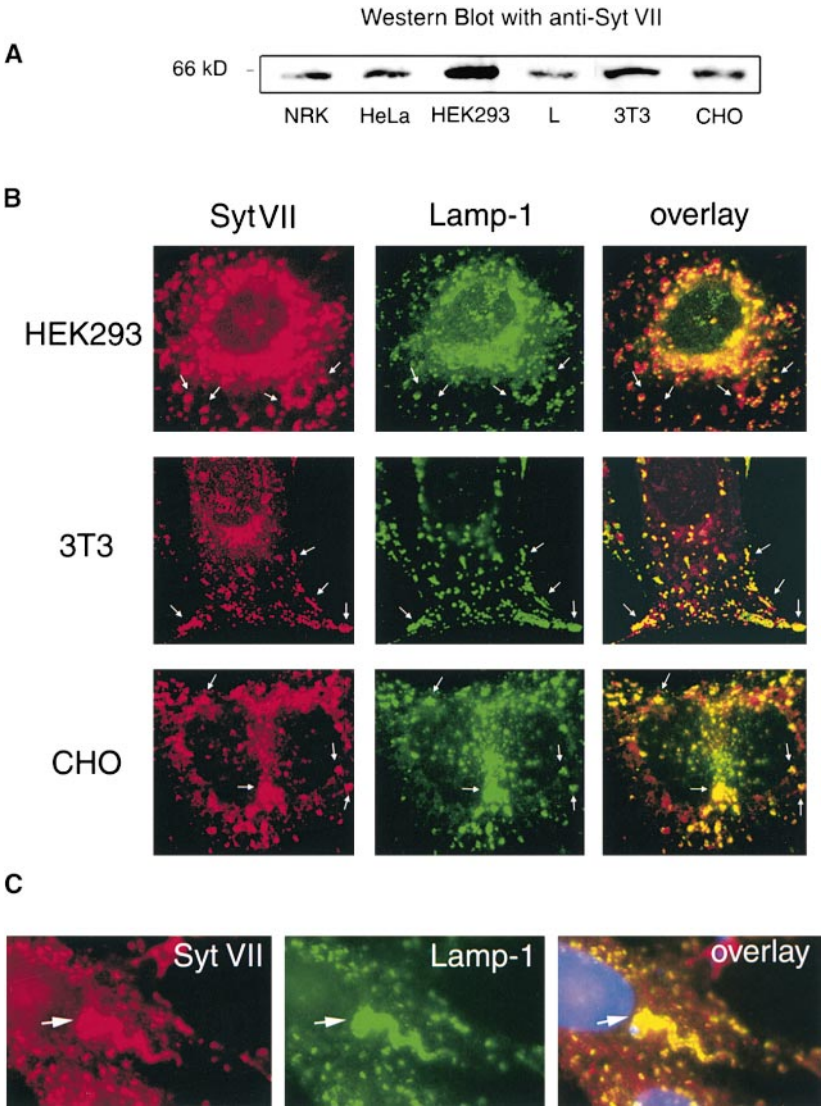

Figure 1. Syt VII is localized on the membranes of lysosomes and of *T. cruzi*–containing intracellular vacuoles. (A) Detection of Syt VII on extracts of different cell types by Western blot using antibodies specific for the unique NH_2-terminal Syt VII ectodomain. (B) Double immunofluorescence showing colocalization of Syt VII (red) and the lysosomal glycoprotein Lamp-1 (green) in HEK-293, 3T3, and CHO cells. Arrows point to examples of compartments double positive for Syt VII and Lamp-1. (C) Double immunofluorescence showing colocalization of Syt VII (red) and Lamp-1 (green) on the membranes of intracellular vacuoles containing *T. cruzi* (arrows). DAPI staining of host cell and parasite DNA is shown in blue.

followed by incubation at 37°C in a 5% CO_2 atmosphere for 1 h before exposure to parasites.

Cell Invasion Assays. *T. cruzi* invasion assays of NRK and CHO cells were performed by exposing cells plated 48 h before (10^4 cells/cm^2) to 5×10^7 trypomastigotes per milliliter in DMEM 2% FBS for 1 h at 37°C. After PBS washes and 2% paraformaldehyde fixation, the number of intracellular and extracellular trypomastigotes associated with cells was determined by immunofluorescence, as previously described (2). For *T. gondii* invasion assays, 5×10^7 parasites per milliliter were added to CHO cells plated as above and incubated at 37°C for 1 h. After PBS washes and fixation in 100% methanol for 1 min, intracellular parasites were quantitated by immunofluorescence using the mAb T62H11 specific for the dense granule protein GRA3, which is incorporated into the parasitophorous vacuole membrane during invasion (25). Invasion and immunofluorescent quantitation of intracellular *S. typhimurium* strain SL1344 after a 30-min infection of CHO cells was done as described (26). In all experiments, cells expressing very high or very low levels of GFP, as determined by fluorescence microscopy examination, were excluded from analysis. In all assays, a minimum of 200 transfected cells was analyzed for each point, and results were normalized to parasites per 100 cells.

Results and Discussion

As mentioned above, *T. cruzi* invades a large variety of vertebrate cells, through a mechanism involving early interaction with host lysosomes. Previous studies showed that the synaptotagmin isoform Syt VII is localized on the membrane of lysosomes of NRK cells, where it regulates Ca^{2+}-triggered exocytosis (8). Thus, to investigate a possible role for Syt VII on *T. cruzi* invasion, it was first necessary to verify if Syt VII was also present on the membranes of lysosomes of additional cell types. A protein with the expected migration in SDS-PAGE for Syt VII (~65 kD) was detected on extracts of different cell types (human, rat, mouse, and hamster) with antibodies against the unique NH_2-terminal domain of Syt VII (Fig. 1 A). In immunofluorescence assays, Syt VII was found to colocalize with the lysosomal marker Lamp-1 in human HEK293, mouse 3T3, hamster CHO (Fig. 1 B), human HeLa, and mouse L cells (not shown). Taken together with the previous detailed characterization of Syt VII expression in NRK cells (8), these results indicate that Syt VII is present on the membranes of lysosomes of a large variety of mammalian cell types. Immunofluorescence of *T. cruzi*–infected CHO cells with specific anti–Syt VII antibodies also demonstrated that this isoform is incorporated into the membranes of recently formed intracellular vacuoles containing trypomastigotes (Fig. 1 C). Very similar images (not shown) were obtained in NRK cells transfected with an expression plasmid encoding full-length Syt VII fused to GFP, previously shown to be targeted to lysosomes (8).

To investigate whether modulation of Syt VII function had an effect on *T. cruzi* invasion, affinity-purified antibodies against the Syt VII C_2A domain were introduced into the cytosol of CHO cells by glass bead loading. In this procedure, wounds created on the plasma membrane by contact with the glass beads are rapidly resealed at 37°C in the presence of Ca^{2+}, trapping extracellularly added molecules inside the cells (24). Previous studies in NRK cells showed that these anti–Syt VII C_2A antibodies, when added to streptolysin O–permeabilized cells, are effective inhibitors of the exocytosis of lysosomes triggered by 1 μM Ca^{2+} (8). As shown in Fig. 2, a marked inhibition was observed on *T. cruzi* invasion of CHO cells loaded with anti–Syt VII C_2A antibodies. Whereas trypomastigotes entered normally unloaded cells or cells loaded with preimmune rabbit IgG, a reduction in the number of intracellular parasites of ~50% was observed in cells preloaded with anti–Syt VII C_2A antibodies (Fig. 2, A–C).

Earlier studies showed that soluble recombinant constructs containing the C_2A domain of Syt VII also inhibit Ca^{2+}-dependent exocytosis of lysosomes in permeabilized

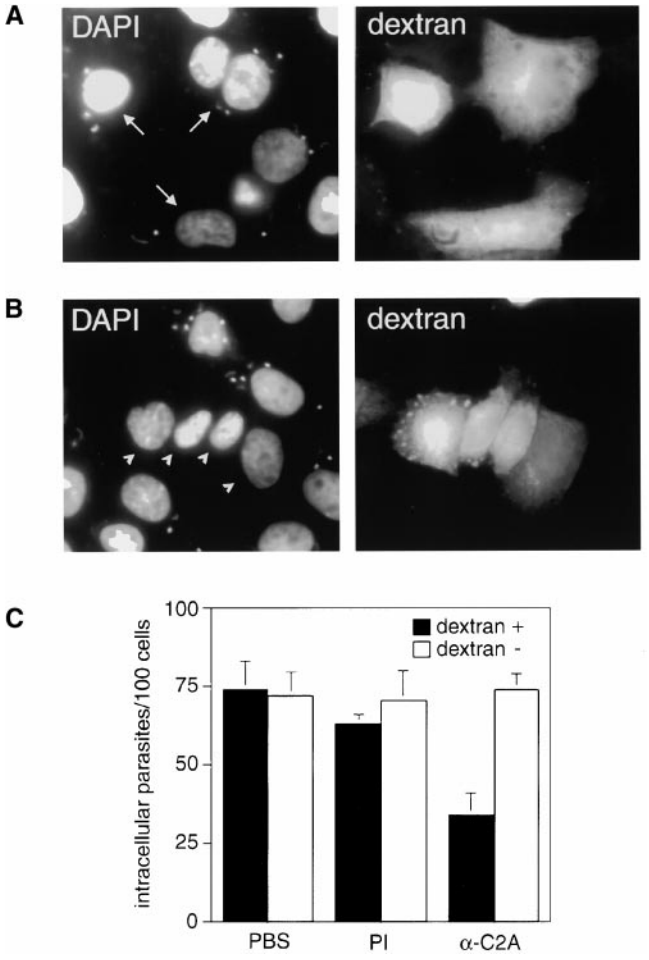

Figure 2. Antibodies against the Syt VII C_2A domain inhibit cell invasion by *T. cruzi*. (A) DAPI DNA stain (left) and Texas Red–dextran (right) fluorescent images of CHO cells loaded with preimmune rabbit IgG. Arrows point to infected cells previously loaded with dextran and IgG. (B) Same as A, except that the cells were loaded with affinity-purified antibodies against the Syt VII C_2A domain. Arrowheads point to uninfected cells previously loaded with dextran and IgG. (C) Quantitation of the number of intracellular trypomastigotes found in cells loaded (black bars) or unloaded (white bars) with dextran, in the presence of PBS only or of preimmune (PI) or anti–Syt VII C_2A antibodies (α-C_2A). The data is expressed as the mean ± SD of triplicate infections.

Table I. *Expression Levels of GFP and Synaptotagmin C_2A–GFP Constructs in Transiently Transfected CHO Cells*

	Average intensity	SD	Intensity range
GFPv	30.7	15.8	14.9–46.5
Syt I C_2A	38.5	17.3	21.2–55.8
Syt VII C_2A	26.2	13.3	12.9–39.5
Syt VIII C_2A	28.1	16.3	11.8–44.4
Syt IX C_2A	20.0	10.3	9.7–30.3
mSyt VII C_2A	29.9	18.2	11.7–48.1

Average fluorescence intensity values correspond to the means of measurements made on images of 40 individual transfected cells, as detailed in Materials and Methods. Background values (subtracted from each fluorescence intensity value) were 22.4 ± 0.5 for cells expressing synaptotagmin C_2A–GFP constructs and 25.9 ± 1.1 for cells expressing the pEGFP-N2 vector alone (GFPv).

cells in a dose-dependent manner. Equivalent constructs containing the C_2A domain of Syt I, the exclusively neuronal isoform, have no effect (8). To verify if a similar effect was observed with *T. cruzi* invasion, CHO cells were transiently transfected with vectors encoding GFP-tagged constructs of Syt I C_2A and Syt VII C_2A or GFP alone. The GFP expression levels 24 h after transfection were determined by image analysis as described in Materials and Methods and found to be within a similar range (Table I). When the number of intracellular trypomastigotes was evaluated, no statistically significant difference was found between the number of intracellular parasites in untransfected and in GFPv- and Syt I C_2A–GFP-transfected cells ($P = 0.7906$, one-way analysis of variance test). In contrast, an extremely significant inhibition of *T. cruzi* entry was observed in Syt VII C_2A–GFP-transfected cells ($P = 0.0001$, unpaired Student's *t* test; Fig. 3 A). Taken together with the inhibitory effect of anti–Syt VII C_2A antibodies (Fig. 2 C), these results strongly suggest that the C_2A domain of Syt VII interferes specifically with the *T. cruzi* cell invasion process, similar to what is observed with Ca^{2+}-triggered exocytosis of lysosomes.

We thus proceeded to verify whether invasion by intracellular pathogens different from *T. cruzi*, which enter host cells by mechanisms not involving Ca^{2+}-dependent lysosome recruitment and fusion, was affected by the Syt VII C_2A domain. CHO cells were transfected with GFPv, Syt I C_2A–GFP, and Syt VII C_2A–GFP and infected with the protozoan parasite *T. gondii* or the enteric bacterial pathogen *S. typhimurium*. *Toxoplasma* enters mammalian cells by a motility-based mechanism, generating a plasma membrane–derived parasitophorous vacuole that does not fuse with lysosomes (27). *Salmonella* triggers extensive actin polymerization and membrane ruffling in host cells, being internalized in macropinocytic vacuoles (26). No significant difference in *T. gondii* invasion levels was detected among cells expressing the three different constructs ($P = 0.8484$; Fig. 3 B). In the *S. typhimurium* invasion assays, a marginally significant ($P = 0.0526$) enhancement in the number of intracellular bacteria (reproducible in several experiments) was observed in cells transfected with Syt VII C_2A–GFP (Fig. 3 C). These findings thus indicate that the mechanism by which Syt VII C_2A reduces host cell suscep-

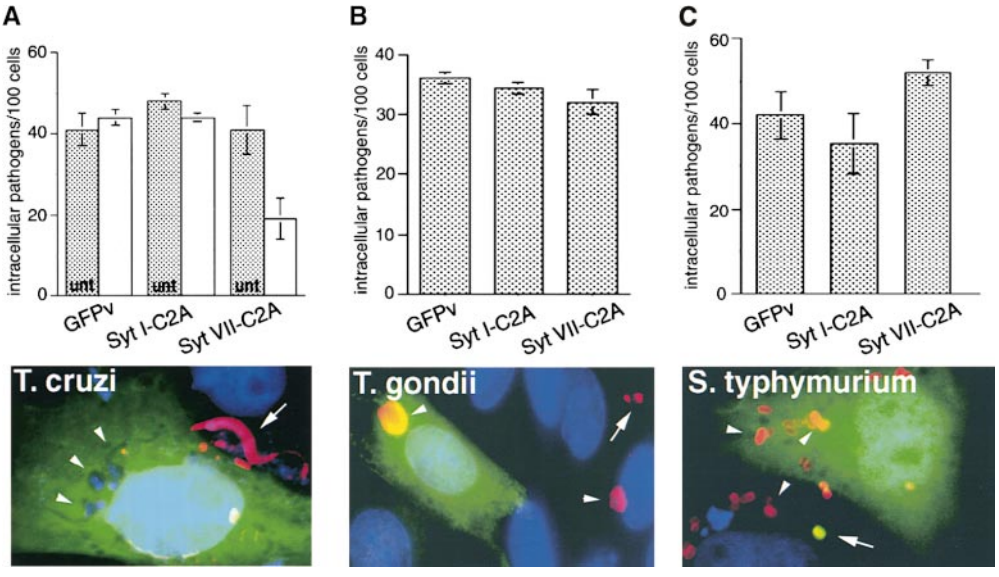

Figure 3. Expression of the Syt VII C_2A domain inhibits cell invasion by *T. cruzi* but not by *T. gondii* or *S. typhimurium*. (A) *T. cruzi* invasion of CHO cells untransfected (gray bars; unt) or transfected (white bars) with GFPv, Syt I C_2A–GFP, and Syt VII C_2A–GFP. (B) *T. gondii* invasion of CHO cells transfected with GFPv, Syt I C_2A–GFP, and Syt VII C_2A–GFP. (C) *S. typhymurium* invasion of CHO cells transfected with GFPv, Syt I C_2A–GFP, and Syt VII C_2A–GFP. The data is expressed as the mean ± SD of triplicate infections. The color images below panels A, B, and C illustrate the immunofluorescence detection assays used to distinguish intracellular and extracellular pathogens: GFP is shown in green, antibodies against *T. cruzi*, *Toxoplasma*, or *Salmonella* in red, and DAPI DNA stain in blue. Arrows point to extracellular organisms and arrowheads to intracellular ones.

tibility to infection by *T. cruzi* is specific for this parasite's invasion strategy and probably directly related to the regulatory role of Syt VII on Ca^{2+}-dependent fusion of lysosomes with the plasma membrane (8).

A similar inhibitory effect of Syt VII C_2A on *T. cruzi* invasion of ~50% was observed in NRK cells transfected with Syt VII C_2A–GFP constructs (Fig. 4 A). These residual levels of parasite entry, also observed in CHO cells loaded with anti–Syt VII C_2A antibodies (Fig. 2 C) or transfected with Syt VII C_2A constructs (Fig. 3 A), could be attributed to either an incomplete inhibition of Syt VII function or to an alternative invasion pathway. Several lines of evidence indicate that an incomplete inhibition of Syt VII function is responsible for this observation. In strong support of this view, when NRK cells were microinjected with his-tagged Syt VII C_2A domain constructs, a markedly stronger inhibition in parasite entry (of ~70%) was observed when compared with cells microinjected with Syt I C_2A (Fig. 4 B). Similar results were obtained with microinjected CHO cells (not shown). These observations suggest that intracellular concentrations of Syt VII C_2A higher than those reached in transiently transfected cells were probably achieved by microinjection. Earlier studies demonstrated that concentrations of Syt VII C_2A as high as 200 μg/ml are required for 80–90% inhibition of lysosome exocytosis in permeabilized NRK cells (8).

Because invasion experiments cannot be performed with permeabilized cells (high K^+-containing intracellular buffers adversely affect trypomastigotes) and it is not possible to precisely determine the intracellular concentration of soluble constructs microinjected or expressed in intact cells, we investigated whether the residual invasion observed in Syt VII C_2A–transfected cells had the hallmarks of lysosome-mediated entry, extensively characterized previously in our laboratory (2). All results indicated that this is the case (not shown). First, the intracellular trypomastigotes found in Syt VII C_2A–transfected cells after short infection periods were inside intracellular compartments containing the lysosomal markers Syt VII and Lamp-1. Second, when the actin cytoskeleton of host cells was disrupted by pretreatment with cytochalasin D, invasion levels of cells expressing GFPv, Syt I–GFP, or Syt VII–GFP were equally increased in ~50–60%. Such enhanced susceptibility to *T. cruzi* infection after cytochalasin D treatment was previously described in several cell types and functionally correlated with facilitated lysosome recruitment and fusion (2, 7). This finding clearly rules out a phagocytic, actin-based alternative invasion mechanism. Third, the intracellular parasites escaped normally from the acidified lysosome-derived vacuoles and replicated in the cytosol (28), regardless of the presence of expressed GFP, Syt I C_2A–GFP, or Syt VII C_2A–GFP in the cells.

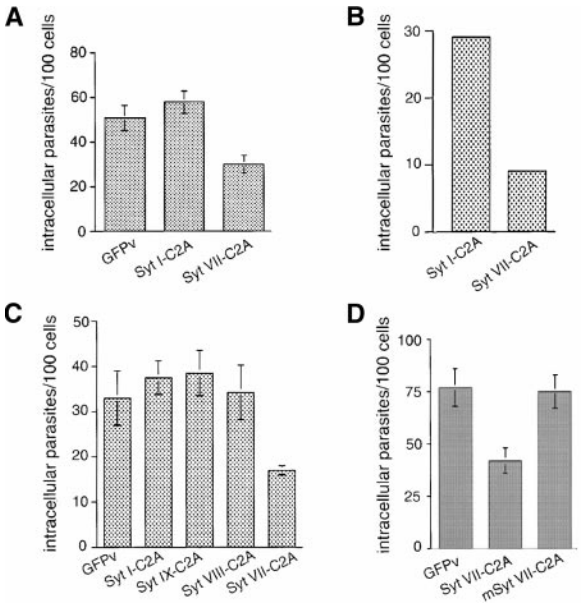

Figure 4. The inhibitory effect on *T. cruzi* invasion is specific for Syt VII and is abolished by mutation of critical C_2A domain residues. The number of intracellular trypomastigotes was quantitated after infection of: (A) NRK cells transfected with GFPv (pEGFP-N2 vector alone), Syt I C_2A–GFP, or Syt VII C_2A–GFP; (B) NRK cells microinjected with his-tagged Syt I C_2A or Syt VII C_2A; (C) CHO cells transfected with GFPv or GFP-fused C_2A domains of the synaptotagmin isoforms Syt I, VII, IX, or VIII; (D) CHO cells transfected with GFPv, Syt VII C_2A–GFP, or mSyt VII C_2A. The data is expressed as the mean ± SD of triplicate infections.

In spite of extensive similarity, characteristic sequence differences exist between the C_2A domains of Syt I and Syt VII (11, 17). Our present and previous (8) results also revealed important functional differences between these domains. The inhibitory effect of Syt VII C_2A and not of Syt I C_2A on both *T. cruzi* invasion and lysosome exocytosis may be related to the previously reported distinct properties exhibited by recombinant forms of these isoforms on protein binding assays. Recombinant Syt I was reported to require Ca^{2+} concentrations in the 200 μM range for binding to syntaxin in vitro, whereas Syt VII–syntaxin interactions were detected at Ca^{2+} concentrations below 10 μM (11). Interestingly, exocytosis of lysosomes, which is specifically inhibited by the C_2A domain of Syt VII, is also triggered at low micromolar $[Ca^{2+}]_i$ (8, 21). A similar differential requirement for $[Ca^{2+}]$ was also reported recently for the interaction of distinct synaptotagmin isoforms with SNAP-25 (12). In addition, Ca^{2+}-dependent oligomerization has been recently proposed to play a central role in the regulation of exocytosis by synaptotagmins (29–31).

To further test the specificity of the inhibitory effect of Syt VII C_2A, we investigated whether the C_2A domains of additional synaptotagmin isoforms endogenously expressed in these cells also influenced *T. cruzi* entry. Specific primers were designed to amplify the C_2A domains of Syt I, II, III, VI, VII, VIII, and IX from NRK and CHO cell mRNA by RT-PCR. In addition to Syt VII, only the C_2A domains of Syt VIII and Syt IX were specifically detected. And as expected, the C_2A domain of the synaptic vesicle–specific isoform Syt I, which is very abundantly expressed in the brain (11), was not amplified from NRK or CHO cell mRNA. Syt VIII was previously detected in several different tissues and defined as a ubiquitously expressed isoform (11, 14). Specific amino acid substitutions that abolish

Ca^{2+} binding were identified in the C_2A domain of Syt VIII, consistent with the lack of Ca^{2+}-dependent binding of this domain to either phospholipids or syntaxin (11, 17, 32). Very little is known about the Syt IX isoform (also referred to as Syt V [reference 14]), except that it appears to be expressed in nonneuronal cells, consistent with our findings (33). When *T. cruzi* invasion assays were performed in CHO cells transiently transfected with C_2A–GFP fusion constructs of Syt I, VII, VIII, and IX, only the Syt VII C_2A domain had a significant inhibitory effect on parasite entry (extremely significant: $P < 0.0001$; Fig. 4 C). The expression levels of all constructs, as determined from the GFP cytosolic fluorescence intensity, were within a similar range (Table I).

The results described above strongly suggested that the C_2A domain of Syt VII has unique properties responsible for both the modulation of *T. cruzi* entry and Ca^{2+}-dependent exocytosis of lysosomes (8). Although the structure of the Syt VII C_2A domain has not yet been solved, the structure of the Syt I C_2A domain is known to consist of an independently folded, eight-stranded β sandwich formed by two four-stranded antiparallel β sheets (34). Structural and biochemical studies showed that Ca^{2+} ions bind at the top of the β sandwich, through five clustered aspartic acid residues, conserved in several Syt isoforms. Interaction with Ca^{2+} does not lead to conformational changes on the C_2A domain of Syt I but instead causes a marked change in the molecule's electrostatic potential, increasing its affinity for effector molecules such as syntaxin and phospholipids (10). It has also been suggested that the unique electrostatic properties of synaptotagmins may allow a positively charged, polybasic region present at the center of both the C_2A and C_2B domains to interact with the negatively charged surface at the core of the SNARE complex, facilitating membrane fusion (35). Indeed, recent studies demonstrated that the polybasic KKKK motif at residues 189–192 of the C_2A domain of Syt I plays a central role in the regulation of Ca^{2+}-triggered exocytosis in PC12 cells. Replacement of these residues by alanines did not interfere with proper folding of the C_2A domain, as indicated by normal interaction with syntaxin and phospholipids in vitro, but reduced its inhibitory activity in dense core granule secretion assays (20). We found that recombinant Syt VII C_2A constructs containing mutations either in the corresponding polybasic motif (K183,184A/H185A/K186A) or in the putative Ca^{2+}-binding aspartic acid residues (D166,172,225,227N) were still inhibitory in β-hexosaminidase secretion assays with streptolysin O–permeabilized NRK cells (unpublished data), reinforcing the conclusion that these amino acid replacements do not appear to interfere with proper folding of the Syt VII C_2A domain. The lack of reduced inhibitory activity after these mutations was not surprising, considering the variation in sequence between the polybasic motif of Syt I and Syt VII C_2A (11), and particularly in view of recent findings indicating that functional Ca^{2+}-binding sites remain in Syt I after mutation of Ca^{2+}-coordinating aspartic acid residues (36). Interestingly, however, when both sets of mutations (K183,184A/H185A/K186A and D166,172,225,227N) were combined, the inhibitory activity of Syt VII C_2A in β-hexosaminidase secretion assays was completely abolished (unpublished data). We therefore cloned this construct with both sets of mutations into the pEGFP-N2 expression vector and analyzed its effect in *T. cruzi* invasion assays with transiently transfected CHO cells. Cells expressing GFP alone, wild-type Syt VII C_2A–GFP, and mSyt VII C_2A within a similar range of fluorescence intensity (Table I) were analyzed for the presence of intracellular *T. cruzi*. As shown in Fig. 4 D, the specific amino acid substitutions on Syt VII C_2A abolished its inhibitory effect on cell invasion by *T. cruzi*, confirming that the mutated residues play similarly important roles in the regulation of lysosomal exocytosis and of *T. cruzi* entry.

Additional studies are required to define the regions of the Syt VII C_2A domain responsible for its unique properties in the regulation of Ca^{2+}-dependent fusion of lysosomes with the plasma membrane. The finding that modulation of Syt VII function affects both Ca^{2+}-regulated exocytosis of lysosomes and the ability of *T. cruzi* trypomastigotes to enter host cells provides, for the first time, a molecular basis for the unusual, lysosome-dependent invasion mechanism of this important pathogen. Taken together, our results strongly suggest that *T. cruzi* subverts the Ca^{2+}-regulated lysosomal exocytic machinery involving Syt VII, which is present in a variety of cell types, as a strategy for cell entry.

We thank Valerian Nakaar, Verena Karsten, and Keith Joiner for reagents and advice with the *Toxoplasma* invasion assays, Sumati Murli and Jorge Galán for help with the *Salmonella* invasion assays, Pietro De Camilli for Syt I plasmids, Anita Reddy for help with the glass bead loading assay, and Henry Tan and Matthew Kelly for excellent technical assistance.

This work was supported by National Institutes of Health grant AI34867 and a Burroughs Wellcome Scholar Award (to N.W. Andrews).

Submitted: 22 December 2000
Revised: 13 March 2001
Accepted: 21 March 2001

References

1. Schenkman, S., E.S. Robbins, and V. Nussenzweig. 1991. Attachment of *Trypanosoma cruzi* to mammalian cells requires parasite energy, and invasion can be independent of the target cell cytoskeleton. *Infect. Immun.* 59:645–654.
2. Tardieux, I., P. Webster, J. Ravesloot, W. Boron, J.A. Lunn, J.E. Heuser, and N.W. Andrews. 1992. Lysosome recruitment and fusion are early events required for trypanosome invasion of mammalian cells. *Cell.* 71:1117–1130.
3. Rodríguez, A., E. Samoff, M.G. Rioult, A. Chung, and N.W. Andrews. 1996. Host cell invasion by trypanosomes requires lysosomes and microtubule/kinesin-mediated transport. *J. Cell Biol.* 134:349–362.
4. Rodríguez, A., M.G. Rioult, A. Ora, and N.W. Andrews. 1995. A trypanosome soluble factor induces IP_3 formation, intracellular Ca^{2+} mobilization, and microfilament rearrangement in host cells. *J. Cell Biol.* 129:1263–1273.

5. Dorta, M.L., A.T. Ferreira, M.E.M. Oshiro, and N. Yoshida. 1995. Ca2+ signal induced by *Trypanosoma cruzi* metacyclic trypomastigote surface molecules implicated in mammalian cell invasion. *Mol. Biochem. Parasitol.* 73:285–289.
6. Moreno, S.N.J., J. Silva, A.E. Vercesi, and R. Docampo. 1994. Cytosolic free calcium elevation in *Trypanosoma cruzi* is required for cell invasion. *J. Exp. Med.* 180:1535–1540.
7. Caler, E.V., S. Vaena de Avalos, P.A. Haynes, N.W. Andrews, and B.A. Burleigh. 1998. Oligopeptidase B-dependent signaling mediates host cell invasion by *Trypanosoma cruzi*. *EMBO (Eur. Mol. Biol. Organ.) J.* 17:4975–4986.
8. Martinez, I., S. Chakrabarti, T. Hellevik, J. Morehead, K. Fowler, and N.W. Andrews. 2000. Synaptotagmin VII regulates Ca^{2+}-dependent exocytosis of lysosomes in fibroblasts. *J. Cell Biol.* 148:1141–1149.
9. Sudhof, T., and J. Rizo. 1996. Synaptotagmins: C2 domain proteins that regulate membrane traffic. *Neuron.* 17:379–388.
10. Schiavo, G., S.L. Osborne, and J.G. Sgouros. 1998. Synaptotagmins: more isoforms than functions? *Biochem. Biophys. Res. Commun.* 248:1–8.
11. Li, C., B. Ulrich, J.Z. Zhang, R.G. Anderson, N. Brose, and T.C. Sudhof. 1995. Ca2+-dependent and independent activities of neural and non-neural synaptotagmins. *Nature.* 375: 594–599.
12. Gerona, R.R.L., E.C. Larsen, J.A. Kowalchyk, and T.F.J. Martin. 2000. The C-terminus of SNAP25 is essential for Ca(2+)-dependent binding of synaptotagmin to SNARE complexes. *J. Biol. Chem.* 275:6328–6336.
13. Sollner, T.H., and J.E. Rothman. 1996. Molecular machinery mediating vesicle budding, docking and fusion. *Cell Struct. Funct.* 21:407–412.
14. Craxton, M., and M. Goedert. 1999. Alternative splicing of synaptotagmins involving transmembrane exon skipping. *FEBS Lett.* 460:417–422.
15. Ullrich, B., and T.C. Sudhof. 1995. Differential distributions of novel synaptotagmins: comparison to synapsins. *Neuropharmacology.* 34:1371–1377.
16. Davis, A.F., J. Bai, D. Fasshauer, M.J. Wolowick, J.L. Lewis, and E.R. Chapman. 1999. Kinetics of synaptotagmin responses to Ca2+ and assembly with the core SNARE complex onto membranes. *Neuron.* 24:363–376.
17. Sugita, S., and T.C. Sudhof. 2000. Specificity of Ca2+-dependent protein interactions mediated by the C2A domains of synaptotagmins. *Biochemistry.* 39:2940–2949.
18. Bommert, K., M.P. Charlton, W.M. DeBello, G.J. Chin, H. Betz, and G.J. Augustine. 1993. Inhibition of neurotransmitter release by C2-domain peptides implicates synaptotagmin in exocytosis. *Nature.* 363:163–165.
19. Mikoshiba, K., M. Fukuda, J.E. Moreira, F.M. Lewis, M. Sugimori, M. Niinobe, and R. Llinas. 1995. Role of the C2A domain of synaptotagmin in transmitter release as determined by specific antibody injection into the squid giant synapse preterminal. *Proc. Natl. Acad. Sci. USA.* 92:10703–10707.
20. Thomas, D.M., and L.A. Elferink. 1998. Functional analysis of the C2A domain of synaptotagmin 1: implications for calcium-regulated secretion. *J. Neurosci.* 18:3511–3520.
21. Rodríguez, A., P. Webster, J. Ortego, and N.W. Andrews. 1997. Lysosomes behave as Ca2+-regulated exocytic vesicles in fibroblasts and epithelial cells. *J. Cell Biol.* 137:93–104.
22. Stinchcombe, J.C., and G. Griffiths. 1999. Regulated secretion from hemopoietic cells. *J. Cell Biol.* 147:1–6.
23. Andrews, N.W. 2000. Regulated secretion of conventional lysosomes. *Trends Cell Biol.* 10:316–321.
24. McNeil, P., and E. Warder. 1987. Glass beads load macromolecules into living cells. *J. Cell Sci.* 88:669–678.
25. Dubremetz, J.F., A. Achbarou, D. Bermudes, and K.A. Joiner. 1993. Kinetics and pattern of organelle exocytosis during *Toxoplasma gondii*/host cell interaction. *Parasitol. Res.* 79:402–408.
26. Hardt, W.D., L.M. Chen, K.E. Schuebel, X.R. Bustelo, and J.E. Galan. 1998. *S. typhimurium* encodes an activator of Rho GTPases that induces membrane ruffling and nuclear responses in host cells. *Cell.* 93:815–826.
27. Dobrowolski, J.M., and L.D. Sibley. 1996. *Toxoplasma* invasion of mammalian cells is powered by the actin cytoskeleton of the parasite. *Cell.* 84:933–939.
28. Ley, V., E.S. Robbins, V. Nussenzweig, and N.W. Andrews. 1990. The exit of *Trypanosoma cruzi* from the phagosome is inhibited by raising the pH of acidic compartments. *J. Exp. Med.* 171:401–413.
29. Littleton, J.T., T.L. Serano, G.M. Rubin, B. Ganetzky, and E.R. Chapman. 1999. Synaptic function modulated by changes in the ratio of synaptotagmin I and IV. *Nature.* 400: 757–760.
30. Bai, J.C., A. Earles, J.L. Lewis, and E.R. Chapman. 2000. Membrane-embedded synaptotagmin penetrates cis or trans target membranes and clusters via a novel mechanism. *J. Biol. Chem.* 275:25427–25435.
31. Fukuda, M., and K. Mikoshiba. 2000. Distinct self-oligomerization activities of synaptotagmin family. Unique calcium-dependent oligomerization properties of synaptotagmin VII. *J. Biol. Chem.* 275:28180–28185.
32. Ullrich, B., C. Li, J.Z. Zhang, H. McMahon, R.G. Anderson, M. Geppert, and T.C. Sudhof. 1994. Functional properties of multiple synaptotagmins in brain. *Neuron.* 13:1281–1291.
33. Hudson, A.W., and M.J. Birnbaum. 1995. Identification of a non-neuronal isoform of synaptotagmin. *Proc. Natl. Acad. Sci. USA.* 92:5895–5899.
34. Sutton, R.B., B.A. Davletov, A.M. Berghuis, T.C. Sudhof, and S.R. Sprang. 1995. Structure of the first C_2 domain of synaptotagmin I: a novel Ca2+-phospholipid-binding fold. *Cell.* 80:929–938.
35. Sutton, R.B., J.A. Ernst, and A.T. Brunger. 1999. Crystal structure of the cytosolic C2A-C2B domains of synaptotagmin III: implications for Ca^{2+}-independent SNARE complex interaction. *J. Cell Biol.* 147:589–598.
36. Fernández-Chacón, R., A. Konigstorfer, S.H. Gerber, J. García, M.F. Matos, C.F. Stevens, N. Brose, J. Rizo, C. Rosenmund, and T.C. Sudhof. 2001. Synaptotagmin I functions as a calcium regulator of release probability. *Nature.* 410:41–49.